Open Access

Recent Progress in Materials

LIDSEN Publishing Inc.

Review

Application of Finite Element Method for Mechanical Characterization of Wood and Reconstituted Lignocellulosic-Based Composites – A Review

Adefemi Adebisi Alade, Ahmed Ibrahim *

Civil and Environmental Engineering Department, University of Idaho, 83844 Moscow, ID, USA; E-Mails: alade@uidaho.edu; aibrahim@uidaho.edu

* **Correspondence:** Ahmed Ibrahim; E-Mail: aibrahim@uidaho.edu

Academic Editor: Mostafa Seifan

Special Issue: New Trends on Construction Technologies and Sustainable Building Materials

Recent Progress in Materials
2023, volume 5, issue 1
doi:10.21926/rpm.2301003

Received: September 22, 2022
Accepted: January 03, 2023
Published: January 09, 2023

Abstract

Performance evaluations of wood and other lignocellulosic-based composites involve complex scenarios of several factors such as material heterogeneity and geometry that often leads to complicated, expensive, and time-consuming experimental procedures. Hence, the application of computational modeling and simulation is desirable to mitigate these biocomposites' performance testing challenges. This review paper, therefore, presents an outlook on the finite element method (FEM) application in probing performance characteristics of wood and solid wood-based composites as well as reconstituted wood and other lignocellulosic-based composites. Notwithstanding the complex nature of wood and other lignocellulosic biomass, the feasibility of FEM application in characterizing their performances has been favorably demonstrated. Going forward, broader applications of FEM combined with the design of experiments would further establish developing protocols. More exploration of FEM-based parametric and optimization studies would facilitate comprehensive, cost-efficient, and swift biocomposites design and performance optimization processes thereby enhancing their acceptance and implementation in target applications.

Keywords

Biocomposites; computational modeling; numerical simulation; finite element analysis

1. Introduction

The exploration of composite materials for various applications that include engineering, biomedical, naval, space, etc. continues to attract interest due to their design flexibility and performance qualities such as high strength-to-weight ratio, thermal and impact resistances, etc., [1-3]. In the last two decades, composite development using reconstituted fibers and particles from wood and plant origin for non-structural and structural components in buildings has exponentially increased. The tremendous increase is attributable to significant efforts geared toward the valorization of lignocellulosic waste streams that include lesser-use small dimension wood [4], wastes from wood processing [1, 5], and agricultural residues such as flax and hemp fibers [6-11]. Likewise, the desire for products with a low carbon footprint towards environmental sustainability and a green economy [8], and the need to replace petroleum-based products with renewable and biodegradable materials as noted by several authors [6, 9, 12-14] continue to promote the exploration of lignocellulosic biomass such as hemp fiber [6, 8, 9, 12, 13] and wood [14] for the manufacturing of bio-based composites. However, to enhance the emerging growth and industry acceptance of wood and lignocellulosic-based composites, the approach by which these composites' characteristics are evaluated must equally be advanced to meet contemporary expectations of a rapid and broad performance evaluation and optimization process.

Muzel et al. [2] pointed out the need for technological advancement in the evaluation and optimization of composite properties. El Houjeyri et al. [14] and O'Loinsigh et al. [15] noted the multi-scenarios of various parameters such as material and geometrical factors involved in experimental programs to determine composite properties. Conducting these comprehensive experimental programs involves high resource costs such as materials and time that are sometimes beyond reasonable and efficiently attainable levels by direct physical testing. Applying computational techniques would alleviate such associated high-cost inputs by reducing the number of required experimental tests [14-16]. Moreover, the heterogeneity of lignocellulosic-based composites owing to the fusion of non-woody and woody materials with different physicochemical properties makes their characterization more challenging [2, 17]. Thus, a resource-efficient approach such as computational modeling and simulation which offers the functionality to obtain a comprehensive understanding of localized and global behaviors of composites is desirable [2, 18]. Furthermore, there are often difficulties in meeting some standard requirements for test sample dimensions or obtaining samples that vary only by a single structural parameter for experimentations as noted in a study by Chen et al. [19]. Such limitations are attributable to the nature of the composite materials and manufacturing process thus compelling researchers to sometimes modify test sample dimension requirements subjectively. These limitations are surmountable with the use of computational models and process simulations to align with established standard requirements. The use of numerical simulation would also ensure that the required precision, accuracy, and process reliability are delivered seamlessly to globally predict the influence of the varied material properties and process conditions on response variables of interest [19].

The approach of computational modeling and process simulation as a non-destructive and resource-efficient method for predicting the behavior of wood and other lignocellulosic-based

composites is gaining more attention. The application of the finite element method (FEM) is playing a significant role in this regard [14, 19, 20]. FEM is a robust numerical method applicable for the analysis of a wide range of engineering problems that include stress analysis, failure analysis, heat transfer, vibration analysis, fluid mechanics, electromagnetism, etc., to obtain approximate solutions [17, 21, 22]. The concept of FEM involves the subdivision of mathematical models for a region of interest into non-intersecting components in a process known as discretization to create finite elements of simpler geometries. Subsequently, a global model response is obtained via an assemblage of the approximate solutions for all the individual finite elements [23]. In essence, finite element analysis (FEA) is a numerical model and simulation-based approach toward predictive solutions for engineering problems wherein the model of an engineering material is discretized into finite elements to obtain localized and global behavior of the material in response to simulated conditions such as stress, thermal, fluid flow or moisture loadings. FEA can be performed using a range of commercial software packages that include ANSYS, GT-STRUDEL, STAAD-PRO, etc., [21, 22]. The software packages are programmed with mathematical functions and constitutive equations that are fundamental to the characteristics of the individual problem being solved [21]. Defining certain material parameters obtainable by experimental testing are also required to simulate the material's behavior. For instance, the application of FEM for structural analysis of a material's behavior requires experimentally determined elastic constants that include Young's modulus of elasticity (E), shear modulus (G), and Poisson's ratio (v) of the material [20]. The required elastic constants depend on the nature of the material as to whether it is isotropic, orthotropic, or anisotropic based on the directional (i.e., longitudinal, radial, and tangential) properties. The properties of isotropic materials are not direction-dependent like the properties of orthotropic and anisotropic materials that differ in different directions. For example, in wood anatomical structure, the longitudinal, radial, and tangential directions are parallel to the grain direction, perpendicular to the grain direction (along a radius of the circular cross-section of the trunk or growth ring), and perpendicular to the grain direction (tangent to the growth ring thus forming a right angle with the radial direction), respectively. Wood properties differ along these directions therefore elastic constants in the different directions are required for numerical simulations. For instance, nine elastic constants i.e., E, G, and v in the three different mutually perpendicular directions (longitudinal, radial, and tangential) are required when considering wood as an orthotropic material whereas twenty-one elastic constants are required when considered as anisotropic. Some of these elastic constants have been reported in the literature for various hardwood and softwood species [16, 24].

Some of the major advantages of FEM application stem from the fact that the FEA procedure enables consideration of the individual peculiarities of the components or layers of a composite [5] and non-destructive manipulation of geometrical configurations to obtain predictive behavior in response to applied stress [25]. Thus, FEM has become a prominent method for analyzing solid structural systems to obtain an advanced understanding of their performance integrity [23, 26-28]. The obtained FEM solutions are validated in a cross-feed comparison with experimental outcomes [17, 29]. The validated models are further applicable in broad and complex scenarios not easily explorable or unattainable by experimental measurements to enable sophisticated, speedy, and less-expensive investigations involving parametric study and design optimization [23, 28, 30]. As such, the possibility of creating and solving multiple simulations using FEM integrated with the design of experiments provides a huge advantage for efficient design optimization pathways [29,

31]. Hence, research efforts have been directed toward the application of FEM for the analysis of numerous properties of wood and wood-based composite that include stress distribution [20, 32], seismic performance [33], wood torrefaction [34], wood drying [35, 36], microwave scattering [37], corner joint strength [28, 38], nonlinear multiphase modeling for inhomogeneous composite material [39], the influence of orientation and intra-ring variation on wood strands [40], fracture behavior [41, 42], viscoelastic-induced crack propagation [43], size effect on mechanical properties [44, 45], etc. Therefore, this review aims to provide a contextual outlook on different scenarios of FEM applications in studying the performance characteristics of wood and solid wood-based composites as well as reconstituted wood and other lignocellulosic-based composites. This would enable information pooling on the advancements in FEM-wood/lignocellulosic-based composite research and development towards advancing established concepts and expanding the FEM application to unexplored scenarios. It is noteworthy that the theories and constitutive laws governing the FEM approach as it applies to wood and other lignocellulosic-based composites are broadly documented in literature such as [2, 21-23, 43, 46-56] and therefore not addressed within the scope of this review.

2. FEM Applications in Analyses of Wood and Solid Wood-Based Composites (SWCs)

FEM application in wood science is relatively low compared to other fields such as aerospace and automobile [23, 30]. This is largely attributable to the heterogeneity of wood which makes it a complex material to model [23, 41, 46] unlike other materials such as plastic, steel, etc. However, a considerable amount of research focusing on the application of FEM in wood product research and development has been carried out and still evolving. Examples of FEM applications in performance evaluation of wood and SWCs include analyses of stress distribution, design configurations and size effect, the effect of moisture loadings on mechanical properties, seismic performance, etc., as discussed hereafter.

3. FEA of Stress Distribution in Wood and SWCs

Wargula et al. [20] conducted 3D model analyses for stress distributions in tension and compression for pine wood samples with moisture contents of 19.9% and 8.74%. The model involved an orthotropic elastic-plastic deformation range using 8-noded linear brick finite elements wherein the lower end of the tension and compression specimens were fixed while kinematic extortions with pre-defined displacements were applied to the upper end of the specimens. The elastic constants used in modeling the elastic behavior were elastic moduli, Poisson's ratios, and shear moduli in the longitudinal, radial, and tangential directions. The elastic moduli and shear moduli, except for the tensile test, were experimentally obtained whereas Poisson's ratios and shear moduli for the tensile test were obtained either directly or estimated from literature data [20, 24, 57]. The yield point that characteristically separates the elastic and plastic regions was obtained by plotting a straight-line tangent to the experimentally-obtained stress-strain curve. The yield point was taken as the point where the stress-strain curve deviated from the tangent by 1%. A 2D model using 4-noded bilinear plane shear quadrilateral finite elements was employed for the analysis of the shear stress wherein an established reference corner point was fixed while the diagonally opposite corner was given kinematic extortion with pre-defined displacement. It is noteworthy that the main goal of these investigations as noted by the authors was to develop models to obtain the

ultimate strength. Mapping of the characteristic behavior was secondary and based on analysis of the stress-strain curve coverage in the range of ±15% error to obtain the convergence of the FEM model with the experimental outcomes. It can be deduced from the results presented by the authors that the tension models did not accurately predict the elastic-plastic behavior and conspicuously underpredicted by 16% and 24% the longitudinal ultimate tensile strengths for the 8.74% and19.9% moisture content pine wood samples, respectively (e.g., Figure 1). The ultimate tensile strengths were less underpredicted, ranging from 2 to 12%, in the radial and tangential directions (e.g., Figure 2). The compression models for the 19.9% moisture content pine wood slightly underpredicted by ≈1% and 4% the ultimate compressive strengths in the longitudinal and radial directions, respectively (e.g., Figure 3), and recorded nearly 100% accuracy in the predicted ultimate tangential compressive strength (Figure 4). On the other hand, the compression models for the 8.74% moisture content pine wood recorded 100% accuracy in the ultimate longitudinal and radial compressive strengths (e.g., Figure 5) but overpredicted by 4.5% the ultimate tangential compressive strength (Figure 6). The findings indicated that, unlike the compression model outcomes, the accuracy of modeling the ultimate tensile strength of the pine wood is more susceptible to moisture-induced variation. Regardless of the moisture content difference, the shear models overpredicted, ranging from 3% to 13%, the shear strengths in all the directional planes (e.g., Figure 7 and Figure 8).

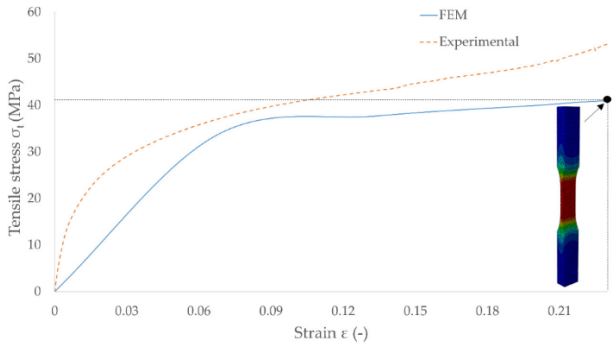

Figure 1 Comparison of FEM model output versus experimental result for longitudinal tensile stress in 19.9% moisture content pine wood. **Source:** Wargula et al. [20]; MDPI | reuse permission CC BY.

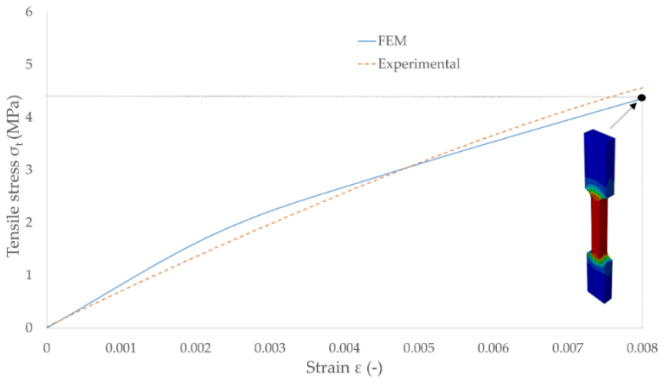

Figure 2 Comparison of FEM model output versus experimental result for radial tensile stress in 8.74% moisture content pine wood. **Source:** Wargula et al. [20]; MDPI | reuse permission CC BY.

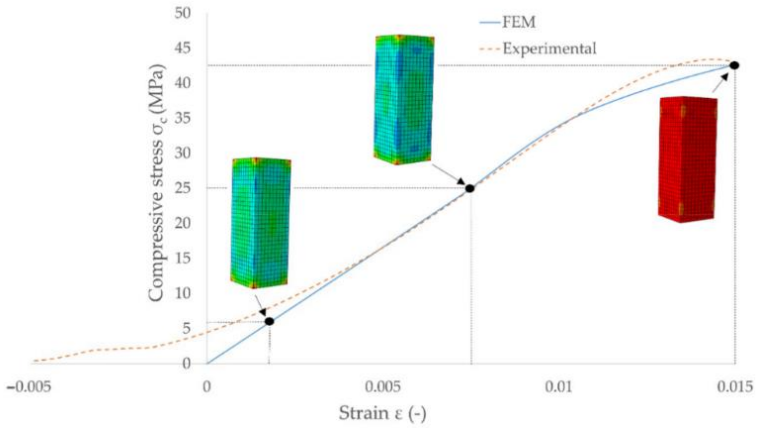

Figure 3 Comparison of FEM model output versus experimental result for longitudinal compressive stress in 19.9% moisture content pine wood. **Source:** Wargula et al. [20]; MDPI | reuse permission CC BY.

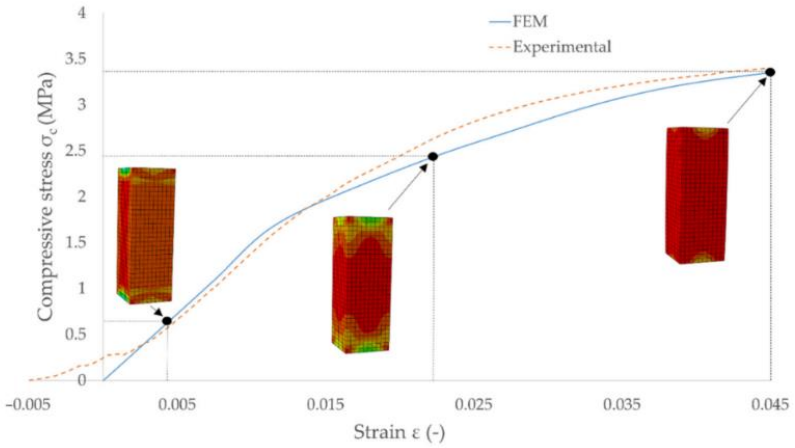

Figure 4 Comparison of FEM model output versus experimental result for tangential compressive stress in 19.9% moisture content pine wood. **Source:** Wargula et al. [20]; MDPI | reuse permission CC BY.

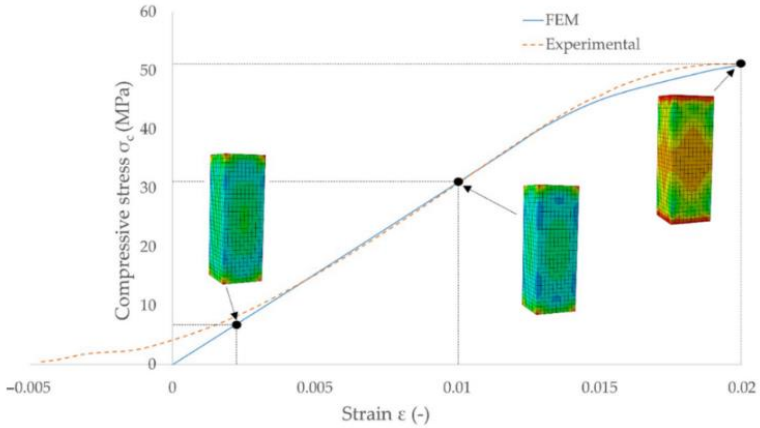

Figure 5 Comparison of FEM model output versus experimental result for longitudinal compressive stress in 8.74% moisture content pine wood. **Source:** Wargula et al. [20]; MDPI | reuse permission CC BY.

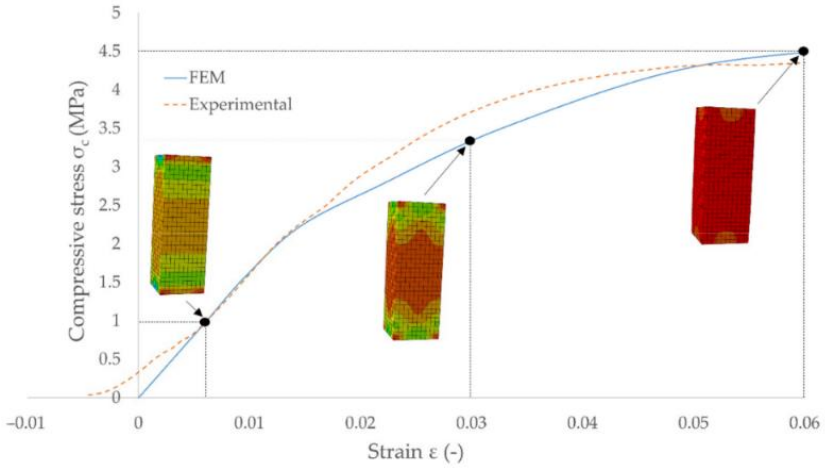

Figure 6 Comparison of FEM model output versus experimental result for tangential compressive stress in 8.74% moisture content pine wood. **Source:** Wargula et al. [20]; MDPI | reuse permission CC BY.

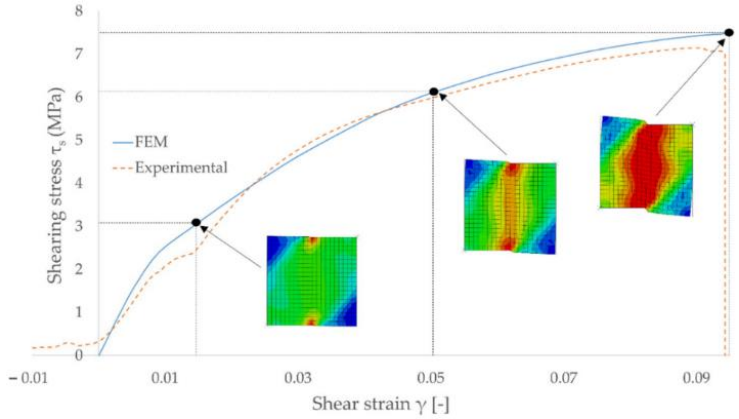

Figure 7 Comparison of FEM model output versus experimental result for longitudinal-radial plane shear stress in 19.9% moisture content pine wood. **Source:** Wargula et al. [20]; MDPI | reuse permission CC BY.

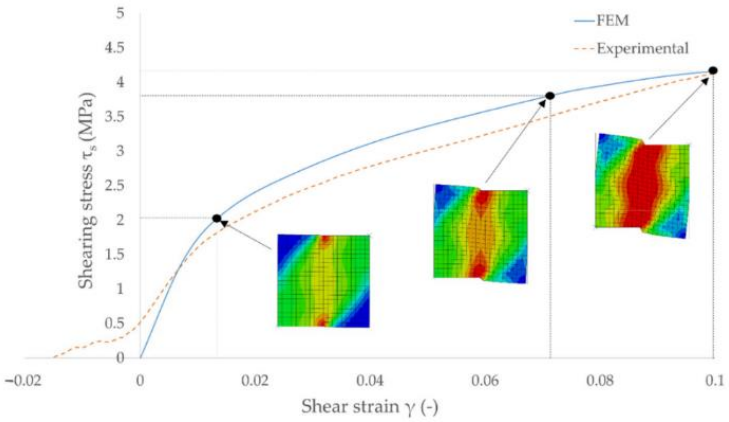

Figure 8 Comparison of FEM model output versus experimental result for radial-tangential plane shear stress in 8.74% moisture content pine wood. **Source:** Wargula et al. [20]; MDPI | reuse permission CC BY.

In summary, the evaluation of maximum stress discrepancies between the finite element models and experimental outcomes showed that the compression model had the best convergence with an error margin of 0 – 5.5% across the longitudinal, radial, and tangential directions. The least convergence was seen in the tension model with an error margin of 2 – 24% while a 3 – 13% error margin was reported for the shear model convergence across the three principal directions. The least model convergence reported in the tension model was probably attributable to the shear moduli which the authors were unable to determine experimentally in their tensile test and therefore adopted literature values. The shear modulus is a measure of a material's stiffness in response to shear stress. Although shear and tensile stresses differ in terms of applied forces, Dahle et al. [58] reported a converging trend that indicated a relationship between shear and tensile strengths of the mushy zone in solidifying aluminum alloys. Likewise, Goulding [59] reported a predictive model for the shear strength of saturated sands as a function of the sum of tensile strength and total normal stress. Notably, depending on the failure (Tresca or von Mises) criterion, the shear strength of metal corresponds to half-fold of its tensile strength or 0.58 of its tensile yield strength [60]. Similarly, the shear strengths of materials like wrought steel, malleable iron, cast iron, copper, and copper alloys, and aluminum and aluminum alloys reportedly correspond to 0.82, 0.90, 1.30, 0.90, and 0.65 of their tensile strengths, respectively [61]. Such referred shear and tensile stress relationships could probably occur in wood material with some degree of interdependency effect. Nonetheless, the tension, compression, and shear models developed by Wargula et al. [20] demonstrated the feasibility of FEM for the mechanical characterization of wood.

Mackerle [27] and Tankut et al. [23] presented bibliographic reviews encompassing a decade of research on the application of FEM in wood analyses. The authors presented literature on topics that include the application of numerical modeling on the anatomical, physical, and mechanical properties of solid wood beams and layered composites for various applications that include trusses, frames, floors, roofs, bridges, etc.; FEA of wood joints including interface and multi-contact simulation, fracture mechanics, modeling of wood drying process, fire resistance performance, and machinability. Other examples of the application of FEM in wood stress analyses include modeling wood-based stair systems to evaluate the structural integrity [30, 62]. Pousette [30] compared experimental and FEA results from an investigation conducted to determine the relationship between prestressing of the center pole and tread displacement in a spiral stair system. The obtained FEA displacements reportedly showed less dependency on the prestress compared to the experimental outcome. The observed differences were attributed to possible effects of wood surface roughness in the tested stair, deformations at tested stair-floor connections, and the assumed perfect connections between the supports and joints of the railing as the latter were not tested in the study. However, the behavioral (structural) response of the stair in the FEA was reportedly the same as that observed in the experiment thus making the model potentially useful for design evaluation in the spiral stair development process. The findings of the study indicated that displacement and structural response should be considered simultaneously in the validation of FE models to determine the model's applicability. The author opined that defining contact elements between all components could produce more accurate modeling of the stair system. Iraola et al. [26] noted that FE models tend to overestimate the elastic behavior of wood connections in a process that is influenced by the contact modeling of the joints thus requiring consideration for singularities at the contacting surfaces. The authors, therefore, proposed and investigated a geometry-based stiffness contact parameter that was found to adequately resolved the

overestimation problem. Much earlier, Jauslin et al. [63] developed a FE model to study the stresses in different wood joints uniaxially loaded in tension with emphasis on contact element modeling to simulate inhomogeneous intrusion (isotropic joint boundary i.e., the glue line) in-between anisotropic adherents. It is noteworthy to mention the complexity associated with experimentally investigating certain wood joints due to intricately linked factors ranging from geometrical such as finger length, width, pitch, and slope to jointing process parameters such as magnitude and duration of applied pressure and adherents-adhesive interface (multiple glue lines in finger joints) to mention a few. Applying their validated FE model, Jauslin et al. [63] were able to conduct a robust parametric study to determine the effects of different joint types (finger, scarf, and step joints), adherents' combination (isotropic, orthotropic, and hybrid), and varied glue line thicknesses (as a function of the joint length) on the stress distribution in the wood joints. Again, this is another scenario in which the application of a FE model would enable a more reliable outcome due to the elimination of probable error inputs like inconsistent configurations as could be nearly inevitable if experimentally investigated.

4. FEA of Design Configuration and Size Effects on Mechanical Properties of Wood and SWCs

The application of FEM in probing the relationship between design parameters and mechanical properties of wood has been explored. Hu et al. [44] investigated the effect of specimen configuration (Figure 9, widths, lengths, and heights all ranging from 10 to 30 mm) on the orthotropic elastic constant properties of European beech wood and the resultant effect on FE simulation outcomes.

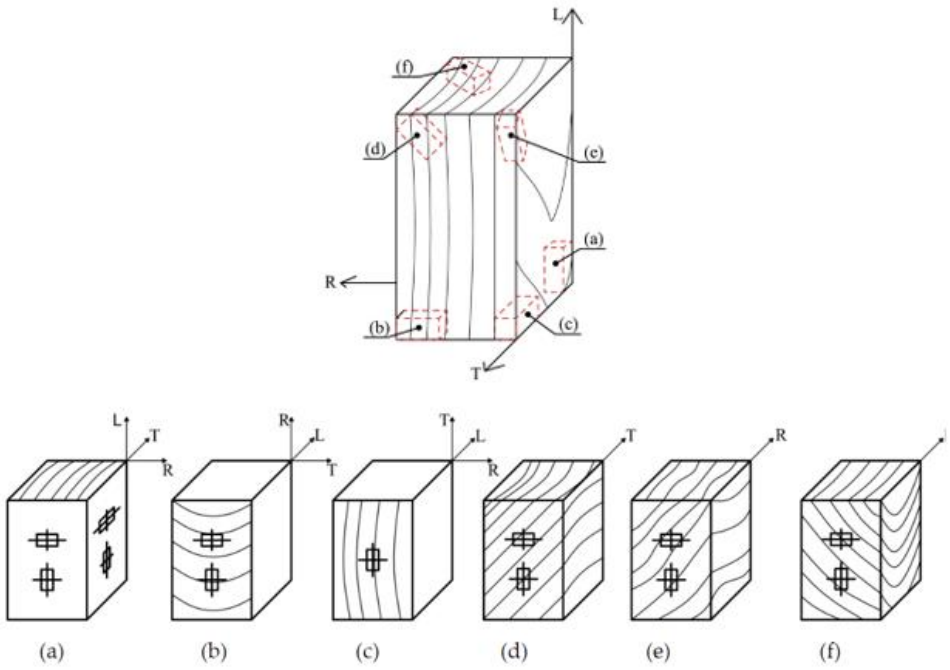

Figure 9 Specimen cutting procedure (top) and configurations (down) for determination of orthotropic elastic constants (i.e., for grain orientations in longitudinal (L), radial (R), and tangential (T) directions). **Source:** Hu et al. [44]; MDPI | reuse permission CC BY.

The authors found that the elastic and shear moduli are directly proportional to the specimen height and inversely proportional to the specimen cross-section area in all three principal axes i.e., longitudinal, radial, and tangential directions. The authors used the elastic constants obtained from five different specimen configurations to simulate the stress distributions in a chair model using FEM (Figure 10). The results obtained by the authors showed that the accuracy of the FEA was influenced by the specimen configuration when compared to the experimental results (Figure 11). The accuracy of the FEA results reportedly decreased with the decrease in the specimen's width-height ratio. The authors also observed that at the same width-height ratio, a smaller specimen dimension yielded a more precise FEA result. The authors noted that the elastic constants obtained from small-dimension specimens yielded more accurate FEA results. The superior FEA accuracy obtained with the smaller specimens was attributed to lesser error due to grain orientation and more uniform mechanics across the specimen volume due to fewer defects. It is noteworthy that the same element type (8-node linear brick – C3D8) and presumably the same element size (not stated by the authors) were used in the FE models for the different specimen configurations. Therefore**,** it would be interesting to determine if mesh refinements in the FEA for the larger specimen configurations could compensate to mitigate the observed effect of a higher width-to-height ratio on the FEA accuracy. Perhaps, establishing a relationship between meshing and specimen configuration could provide better FEA implementation considering the uniqueness of wood and other lignocellulosic fibers. Eslami et al. [53] reported that meshing significantly influenced the softening stage of a modeled timber behavior. Besides, numerical solutions from FE simulations are mesh-dependent [14] thus it is crucial to adopt finite elements that will perform well under convoluted stress states [41].

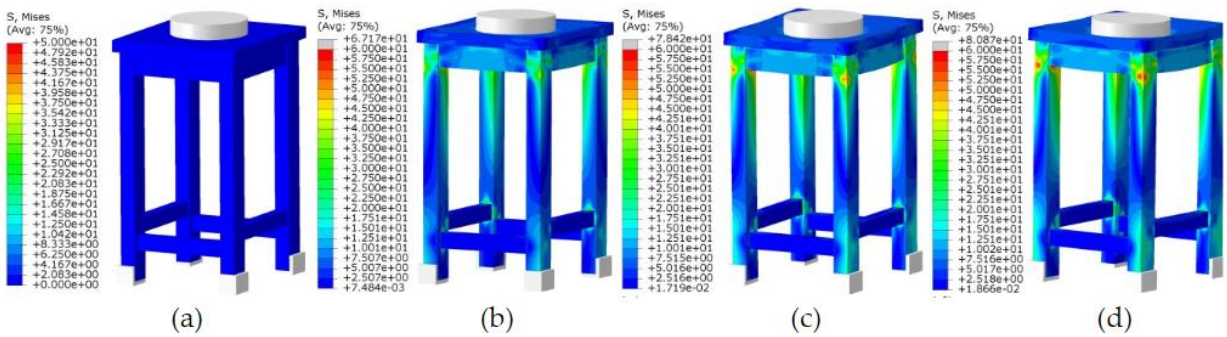

Figure 10 FEA results of stress distribution states in chair model at (a) zero, (b) 1 mm, (c) 2 mm, and (d) 3 mm displacements. **Source:** Hu et al. [44]; MDPI | reuse permission CC BY.

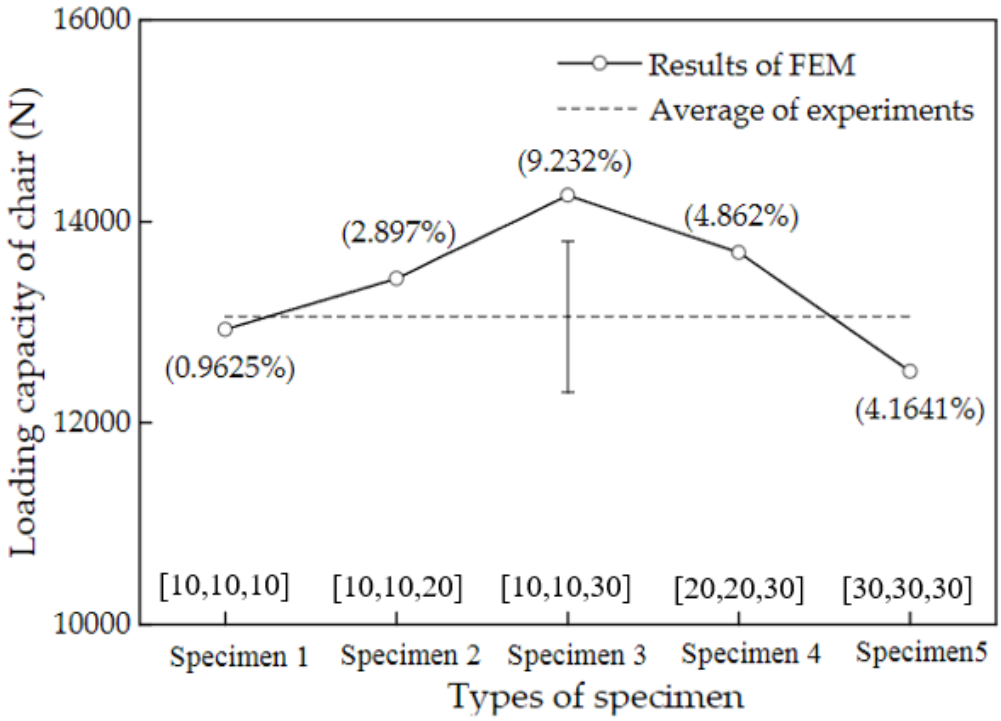

Figure 11 FEM versus experimental outcomes of loading capacities (errors in parentheses) of chair modeled using elastic constants obtained from different specimen configurations. Configurations in square brackets [width, length, height]. **Source:** Adapted from Hu et al. [44]; MDPI | reuse permission CC BY.

In a different study, El Houjeyri et al. [14] used an orthotropic elastoplastic FE model to predict the non-linear behavior and failure mode of adhesive-free laminated and cross-laminated oak wood composites. After validation, the authors further employed the developed FE model to determine the influence of design parameters that include layer number, connector (dowel) spacing, dowel diameter, and inclination angle of the dowels on the stiffness and strength of the laminated beam. In the first part of their investigations, the authors reported that the developed FE model for a 3-point bending test simulation predicted well the material's nonlinearity, ultimate load-bearing capacity, and mode and growth of failure in the composite beam. Furthermore, the authors reported good agreement of the load-deflection curves and failure modes that include tension failure and layer separation obtained from simulated and experimental-based four-point bending tests. The behavioral response of the laminates based on the FE model in the parametric study reportedly coincides with the experimental occurrence of dowel pull-out as loading increases thus demonstrating the accuracy of FEA in predicting the flexural behavior of the laminates. Similarly, Fajdiga et al. [42] applied computational simulation of a three-point bending test using FEM in studying the mechanical properties of spruce wood in radial and tangential orientations based on an orthotropic material model with damage evolution. The developed FE model provided an accurate prediction of the fracture behavior for the spruce wood specimens. The force versus displacement curves obtained from the computational model and actual experiments (Figure 12) reportedly had correlation coefficients of 0.99 for both radially and tangentially oriented spruce wood specimens. The validated model was presented as applicable in further studies on wood fatigue behavior using numerical simulations.

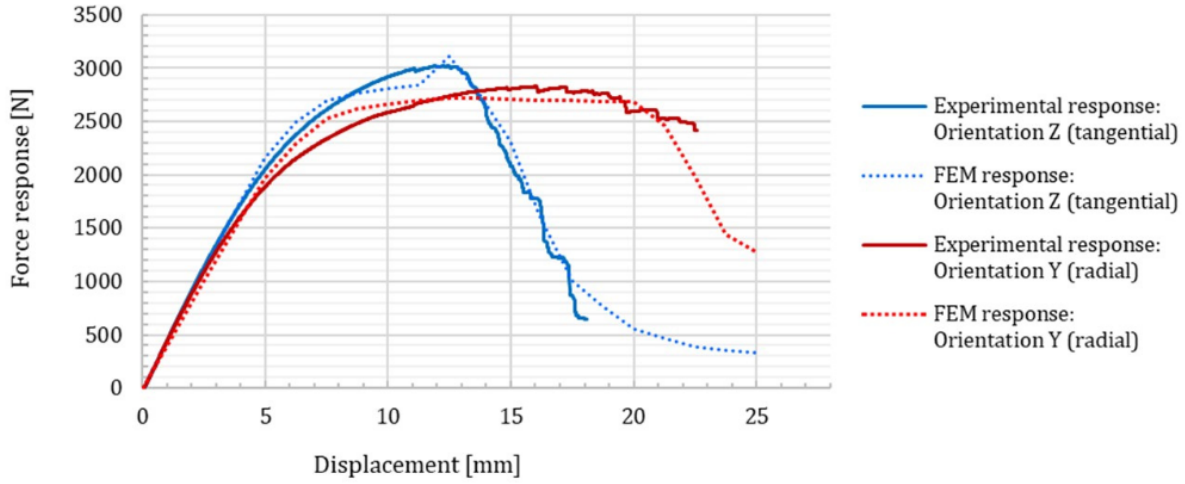

Figure 12 Comparison of FEM versus experimental force-displacement curves obtained from the three-point bending test of spruce wood. **Source**: Fajdiga et al. [42]; MDPI | reuse permission CC BY.

Elsewhere, Xue et al. [64] established the use of FEM in evaluating the seismic behavior of straight-tenon joints in timber buildings. The authors further employed the validated model to conduct a parametric study of the tenon joints to obtain more information on the effect of size, material property, and frictional coefficient on the seismic performance of the tenon joint.

5. FEA of Wood Moisture Effect on Mechanical Properties of Wood and SWCs

The effect of varied physical properties of wood on its mechanical behavior has also been studied using FEM. Autengruber et al. [65] developed a FE simulation concept to enhance the knowledge of failure mechanism in composite I-joist beams made of spruce wood flanges and particleboard web under varying loads and climatic conditions, and for optimization of the cross-section. The authors employed an advanced moisture transport model and multi-surface failure criterion to simulate the moisture-related and brittle failure mechanisms, respectively. Fu et al. [66] established the feasibility of evaluating the compressive performance of beech wood at various moisture levels ranging from 5% to 60% using FEM. The use of FEM enabled the authors to overcome complications that would otherwise be associated with the experimental determination of mechanical functions of the beech wood at different moisture loadings. The moisture-induced trend of the FEA compressive force-displacement curves reportedly showed good consistency with the experimentally observed plasticity of the beech wood as tested in longitudinal, radial, and tangential directions (Figure 13). Thus, the FE model adequately predicted the influence of moisture on the compressive performance of the beech wood. Presumably, the negative displacement values for the FEM results presented in Figure 13 suggest that the authors employed negative force values to indicate directionality for the compression simulation which would resultantly produce negative displacement values. Perhaps, for comparative and ease of visualization purposes, the authors presented only the FEM displacement values in the negative form to avoid a crowded overlap of FEM and experimental curves, considering that multiple curves were presented in the same graph panel. On the other hand, the FEM force values were presented in positive form for ease of

comparison of FEM versus experimental force values. It should therefore be noted that the negative sign in the FEM displacement values does not imply the degree of magnitude rather it implies directionality of the magnitude with respect to the coordinate system during the simulation process.

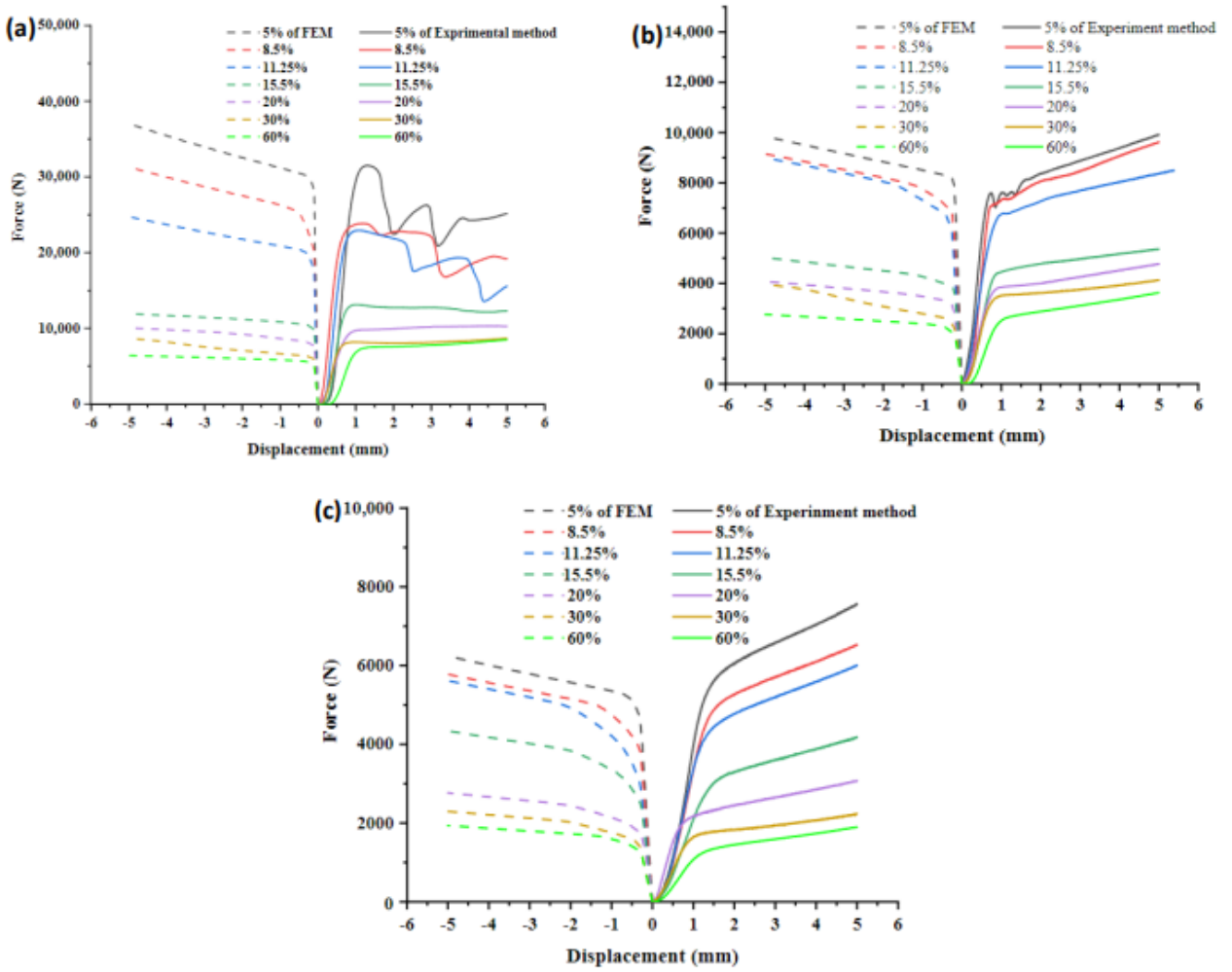

Figure 13 Comparison of FEM and experimental compressive force versus displacement curves at varied moisture loading percentages in beech wood tested at (a) longitudinal, (b) radial, and (c) tangential grain orientations. **Source:** Fu et al. [66]; MDPI | reuse permission CC BY.

Fu et al. [66] further noted that the recorded FEA-experimental error range (0.49% to 16.10%) for the compressive yield strengths across the different moisture levels and grain directions indicated the suitability of the FEM in simulating the elastoplastic behavior of beech wood in compression at multi-moisture levels.

6. Other Examples of FEA of Wood and SWCs Properties

Microwave scanning for the determination of the internal physical properties of wood has been simulated using the FEM approach. Hansson et al. [37] used FEM to analyze the scattering of microwaves in Scot's pine wood. Measurements obtained from a microwave scanner were used to validate the FE model. Both results reportedly corresponded well, however, the authors noted that

the needed computational power in the simulation is directly proportional to the discontinuity in the wood properties that include density and moisture content. Xue et al. [64] conducted FEA on the seismic performance of frame and frame brace made of glued-laminated Douglas fir wood in a structural system that includes steel slab components validated against experimental analysis. The authors reported that the ultimate bearing capacity obtained from the FEA closely agreed with the experimental results. However, the FEA slightly overestimated the strengths of the frame and frame brace attributable to a lack of consideration for in-between components gap, damage evolution, and material dispersion.

Examples of other investigations where FEM reportedly produced predictions that corresponded well with experimental outcomes include the evaluation of mechanical behaviors of timber beams and joints by Khorsandnia et al. [54] and multi-layered wooden beams with welded-through wood dowel by O'Loinsigh et al. [15], load-slip behavior of nailed wood joints under cyclic loading by Chui et al. [67], failure analysis of timber in bending, tension, and compression states by Eslami et al. [53], strength properties of laminated veneer lumber in flat and edge-wise bending by Gilbert et al. [68], non-linear flexural behavior of cross-insulated timber panel with polyurethane foam core by Santos et al. [69], flexural behaviors of glulam timber arches by Smidova et al. [70] and hybrid timber beams by Tran et al. [51], and strength analysis of pine and beech wood dowel and tenon corner joints by Kaygin et al. [28] to name a few.

7. FEM Applications in Analyses of Reconstituted Lignocellulosic-Based Composites (RLCs)

RLCs such as oriented strand board, flakeboard, fiberboard, and particleboard are formed by the agglomeration of strands, flakes, fibers, and particles obtained from wood and non-woody lignocellulosic biomass. Wood deficits have increased interest in the use of non-woody lignocellulosic biomass as well as waste products from wood and non-woody materials for manufacturing composite products [4]. RLCs offer better flexibility than solid wood in terms of controllable properties during processing [17]. Consequently, if the process parameters are properly aligned, reconstituted composites could sometimes offer end products with physical or mechanical properties surpassing those from solid wood [17]. Currently, there is an upward shift in interest concerning the use of RLCs in building components like the roof, wall, and floor elements. However, the intricately linked influence of many factors, ranging from compositional to geometrical, on the properties of reconstituted composites makes their design for specific applications challenging and experimentally costly [18]. Furthermore, the limited resource base of some of the biomass emerging as raw material for composite manufacture and the consequent exploration of fast-growing crops [4] signals the possibility of incorporating different materials to meet industrial demand which would further complicate the experimental evaluation of the final composite properties. For instance, in an evolving trend as an alternative to conventional composite materials, fibers of wood and agricultural residue origins are being integrated to manufacture what could be regarded as wood-non-wood hybrid composites [17]. Therefore, technological advancement in research and development could enhance the implementation of various lignocellulosic biomass as raw materials for composite manufacture [4]. More specifically, the complexities associated with the mechanical characterization of reconstituted composites due to their heterogeneous nature and configurations are surmountable with the use of computational simulation techniques such as the finite element method [2]. For example, Suo and Bowyer [18] noted that computational modeling and simulation

offer a precise characterization of particleboard properties at levels acceptable for research and production purposes. Wong et al. [71] studied the effect of different density profiles on the bending modulus of elasticity for particleboard made from *Shorea spp* and isocyanate resin using FE models. The use of FEM as noted by the authors enabled the evaluation of specific profile portion(s) as a sole factor which otherwise is difficult to achieve experimentally without considering the interaction effect of other influencing factors. In a reliability test performed by the authors to validate the FE model, less than 5% deviation was recorded when the calculated modulus of elasticity based on the FE model was compared to the experimental outcome thus indicating a reasonably good model fit. Other notable FEM studies involving reconstituted composites are presented hereafter.

8. FEA of Mechanical Properties of RLCs

Diaz et al. [17] applied FEM to study the structural behavior of prefabricated thin-walled roof panel composite with sheathing (finish side) made of oriented strand board, a rigid core made of extruded polystyrene, and an external side made of waterproof agglomerate. The authors reported that in most cases the FEM simulation provided good agreement with the experimental results. The contacts of the support elements and material orthotropic nature reportedly posed the highest difficulties for the FEM modeling. Contacts between materials should be modeled in line with the product design and observed response during the experimentation phase. For example, in the absence of noticeable de-bonding between layers or materials, the contact elements could be assumed and modeled as perfectly bonded. Likewise, appropriately defining material properties (i.e., isotropic, orthotropic, or anisotropic) would enable improved accuracy of the FE model and the predicted response [25]. Diaz et al. [17] further suggested that the observed differences between the FEM and experimental outcomes, where applicable, could be linked to the occurrence of failure modes like creep, local buckling, etc. According to Wong et al. [1], increasing sheathing thickness mitigates the susceptibility to buckling failure but thicker outer layers could also experience complex failure modes. Therefore, establishing appropriate specimen/layer thickness could be vital to achieving agreement between experimental and numerical simulation results. Diaz et al. [17] also emphasized the importance of selecting the appropriate mathematical model as it influences the FEM's predicted output. More recently, Hao et al. [72] applied FEM to simulate the impact resistance to windborne debris of insulated panels made of oriented strand board sheathings and expanded polystyrene foam core. The developed model reportedly provided reliable predictions when validated against the experimental test for responses that include failure modes at different projectile impacts, projectile penetration, displacement, and strain on the sheathing. However, the authors reported the sensitivity of the model's convergence to meshing in the region of impact thus supporting the earlier-mentioned statement that FE solutions are mesh-dependent [14]. Therefore, it is important to establish and apply the appropriate element sizing and physics preference to obtain more accurate predictions from FE simulations.

In a different scenario, Labans and Kalnins [73] used a FE model validated against an experimental 4-point bending test to optimize the cross-section parameters of plywood sandwich panels with corrugated core for optimal weight/stiffness designs. During the model validation, the authors attributed the observed higher shear strains in the model prediction probably due to the imprecise setting of the strain measuring angle or inconsistent veneer orientation in the plywood sandwich panels. Thus, giving credence to the importance of identifying the unidirectional properties on the

accuracy of the parametric model as earlier noted by the authors. Chen et al. [19] applied FEM to study the mechanical properties of paper honeycomb-wood composites made of different panel structures (expanded, laminated, or corrugated honeycomb core sandwiched in-between hardboard, medium density fiberboard, or plywood outer layers) and at varied configurations (15.9 mm – 31.8 mm core cell size, 3 mm and 6 mm outer layer thickness, and 0.13 mm – 0.23 mm web thickness). When considering the overall outcome, the FE models reportedly produced results in good agreement with the experimental outcomes. However, instances of clear divergences were observed between the results. Some of the FE models significantly overpredicted (i.e., beyond reasonable error margins of ±5%) the modulus of elasticity as determined under edgewise compression, and overpredicted the interlaminar shear moduli. The observed discrepancies were linked to either measurement errors or bonding defects. This emphasizes the importance of ensuring precision and accuracy as much as possible during the experimental procedures to close ranks with the precision level of the FE models. Mohammadabadi et al. [74] also developed FE models to study the behavioral elasticity of wood-strand composite sandwich panels fabricated using lodgepole and ponderosa pine with a biaxial corrugated core. In comparison to the experimental results, the bending stiffness obtained from the FE model reportedly varied by 6.5% which is slightly higher than the acceptable engineering error margin of ±5%. The FE model reportedly showed less deformation compared to the experimental observation attributable to the modeling of the contact area between the core and face layers using a rigid link that remains undeformed during the FE simulation. The reported outcome affirms the importance of contact modeling to the accuracy of FEA. The material properties used for the FE simulation of the flexural test were obtained from the results of tensile testing of a 640 kg/m^3 panel specimen. Considering the existential density variations between panels or specimens from the same panel, particularly for wood-based materials, the observed difference between the experimental and FEA results is attributable to the possible effect of variation in material properties as alluded to by the authors. It is therefore imperative that the requisite material properties for developing FE models are obtained from the actual experiment to be simulated.

9. FEA of RLCs Made from Nanomaterials

Mechanical characterization using the FEM approach has been applied in studies involving nanomaterial-based composites. Webo et al. [75] developed FE models to predict the flexural properties of mono and hybrid nanocomposites made from sisal nanocellulose fibers and rice husk nanoparticles at different fiber volume fractions with an epoxy resin binder. The experimentally found relationship between the flexural strength and fiber volume fraction of the sisal nanofiber composites (R^2 = 0.98) was accurately predicted by the developed FE model ($R^2 \approx 1.00$). However, the FEA overpredicted the flexural strength of the sisal nanofiber-reinforced composite compared to the experimental results. Providing additional insights into the results presented by these authors, negligible deviations (within an acceptable error margin of ±5%) were recorded between the experimental and FEA results obtained for 30% of the sisal nanofiber-based composites investigated. The acceptable experimental-FEA margins were found above 7% fiber volume fraction. For the rice husk nanoparticle composites, there was a higher flexural strength-fiber volume fraction correlation margin between the experimental (R^2 = 0.98) and FE model-predicted (R^2 = 0.94) results. The recorded difference is attributable to a much earlier initiated but steady decline that is

discernible in the FEA-based flexural strength with an increase in the fiber volume ratio. On the other hand, the experimentally obtained flexural strength continued to rise to more than 150% increment in fiber volume fraction beyond the threshold point occurrence in the FE simulations. However, negligible deviations occurred in 40% of the rice husk nanoparticle-based composites investigated which is higher than that observed in the sisal nanofiber composites despite the better correlation reported in the latter. The acceptable experimental-FEA error margins for the rice husk nanoparticle composites were recorded in the range of 2.69% to 4.71%, and 11.20% fiber volume fraction. For the sisal/rice husk hybrid composites, a relatively perfect agreement was obtained in the flexural strength-fiber volume fraction correlation (R^2 = 0.97) obtained for both experimental and FEA outcomes. However, an earlier but steadier decline could also be noticed at the threshold where the FEA-based flexural strength began to decrease with an increase in fiber volume fraction whereas this threshold scenario occurred after a further 48% increase in fiber volume fraction for the experimental results. Acceptable error margin (within ±5%) between experimental and FEA flexural strength results occurred in about 50% of the sisal/rice husk hybrid-based composites investigated which is greater than the percentages (30% and 40%) occurring in the sisal nanofiber and rice husk nanoparticle mono composites, respectively. The influence of the fiber volume fraction could not be directly related to the reported error margins. A wider correlation margin and deviations between the experimental and FEA results were reported for the flexural stiffness of the mono and hybrid composites. The findings of the study as reclassified above indicate that the FE models provided a better overall factor-response correlation in nanofiber than nanoparticle composites subject to the lignocellulosic material source. On the other hand, deviations between experimental and FEA results were lower in the nanoparticle compared to nanofiber composites. This suggests that the size and origin of the lignocellulosic material used in the composite formulation could influence the FE modeling accuracy and should be considered in the numerical simulation of reconstituted lignocellulosic composites. A major shortcoming in the reporting of the above study was that the authors did not provide some vital details pertinent to the outcome of the numerical simulation such as the model type (although an orthotropic model could be assumed based on some of the elastic constants provided) and geometry. Likewise, the authors did not report the experimental procedures used to obtain the elastic constants of the nanomaterials (which could be very complicated). The availability of such information would benefit future studies, particularly for repeatability and comparative purposes. In another study by the same authors [76], FEA was applied to study the tensile properties of the mono and hybrid composites of sisal nanofibers and rice husk nanosilica particles. The experimental and FEA results reportedly showed an agreement of an increase in the tensile strength to an optimal point and a successive decline afterward for the sisal nanofibers, rice husk nanoparticles, and the hybrid reinforced composites. Tensile strength threshold points were noticeable at fiber volume fractions of approximately 5.24% and 9.04% (for sisal nanofiber reinforced-epoxy resin composites), 5.03% and 6.97% (for rice husk nanoparticle reinforced-epoxy resin composites), and 5.03% and 5.82% (for sisal/rice husk hybrid reinforced-epoxy resin nanocomposites) based on the FEA and experimental results, respectively. Compared to the experimental results, the FEA overestimated the tensile strength of the sisal nanofiber reinforced-epoxy resin composites up to its threshold point but underestimated the tensile strength when considering the region above the threshold point. However, about 36% of the recorded error margin of experimental and FEA results were within acceptable limits of ±5%. Contrary to the earlier discussed flexural strength study, instances of the acceptable experimental-FEA error margin for the

tensile strength occurred at fiber volume fractions less than 7%. From approximately 8% to 12% fiber volume fraction, the error margin of experimental and FEA results ranged from -19.23% to -22.61%. For the rice husk nanoparticle reinforced-epoxy resin composites, the FEA overestimated and underestimated the tensile strength below and above (except at the maximum investigated, ≈ 10%, fiber volume fraction) the threshold point, respectively. About 64% of the recorded error margin of experimental and FEA results for the rice husk nanoparticle-based composites were within the acceptable ±5% limit. For the sisal/rice husk hybrid reinforced-epoxy resin composite, the FEA reportedly overestimated and underestimated the tensile strength up to the threshold point and above (except at 6.97%), respectively. About 45% of the recorded error margin of experimental and FEA results for the sisal/rice husk hybrid-based composites were within the acceptable limit of ±5% and less related to the influence of the fiber volume fraction. The reported variations between the experimental and FEA results were attributed to the levels of accuracy between the methods. Besides, linearization status should also be considered a major influential factor. In modeling reconstituted wood-based composites, result variation due to material non-linearity is surmountable by applying multi-linear function adjustments for the stress-strain relationship as reported by Soriano et al. [5]. The authors suggested consideration of the elastic-linear behavior up to 60% of the ultimate stress. Again, Webo et al. [76] did not disclose the experimental procedures by which the properties of the nanomaterials in this study were obtained. Furthermore, no explanation was provided for the relatively weak tensile properties of the manufactured composites, particularly when considering the properties of the matrix used. Identifying probable factors e.g., material modification or process conditions responsible for such outcomes would be vital in optimizing the strength properties of the composites. Hence, emphasis should be placed on such observations in future studies.

10. Other Examples of FEA of RLCs Properties

Investigations on the application of FEM to study banana fiber-reinforced composites have been conducted by various researchers. These studies include the relationship between fiber loading and mechanical properties of banana-reinforced epoxy composite [77], fracture analysis of banana fiber reinforced-cashew nutshell liquid composite [78], mechanical characterization of banana fiber epoxy reinforced composite [79, 80], coconut coir-banana fiber hybrid reinforced epoxy composites [81, 82], woven banana fiber textile reinforced composite [83], and banana-carbon fiber hybrid composites [84]. A common outcome obtained from these studies is a high-reliability level of the FEA results when validated against experimental outcomes thus establishing the suitability of FEM for evaluating the characteristics and performance of banana fiber composites. However, the minor variations encountered between the FEA and experimental results were attributed to porosity, anisotropy, and fiber-matrix interphase properties [77]. Other notable examples of characteristic evaluation of reconstituted lignocellulosic composites wherein the use of FEM has been established to produce results in good agreement with experimental outcomes include the evaluation of mechanical behaviors of plywood board timber connections [31], tensile and bending strength properties of sandwiched MDF laminated panels [85], and hygromechanical deformation of MDF panel [86].

11. Conclusion

The sole traditional prototype testing of wood and lignocellulosic-based composites cannot fulfill the rapid and comprehensive investigation requirement for contemporary research and product development. Thus, advancing the design and performance optimization processes for these biocomposites by integrating computational modeling and simulation methods such as FEM with experimental investigations is crucial to meet emerging demands for timely, less costly, and in-depth performance assessment protocols. Notwithstanding the complex nature of wood and other lignocellulosic biomass, the feasibility of FEM application in their performance characterization has been favorably demonstrated over a range of responses that include stress distribution, failure analysis, the effect of physical properties on mechanical performance, etc. Going forward, more applications of FEM should be combined with the design of experiments in investigating the properties of wood and lignocellulosic-based composites to further establish the developing protocols and expand into more parametric and optimization studies to deliver sophisticated design and performance evaluation processes. Substantial achievements in this regard would drive enhanced acceptance and implementation of emerging bio-based composites in target applications.

Acknowledgments

This review is part of a research project funded by the National Science Foundation (Grant number: 2119809), USA.

Author Contributions

Dr. A. A. Alade: Conceptualization; Writing – Original draft; Writing – review and editing. **Prof. A. Ibrahim**: Conceptualization; Writing – review and editing.

Competing Interests

The authors have declared that no competing interests exist.

References

1. Wong YJ, Mustapha KB, Shimizu Y, Kamiya A, Arumugasamy SK. Development of surrogate predictive models for the nonlinear elasto-plastic response of medium density fibreboard-based sandwich structures. Int J Lightweight Mater Manuf. 2021; 4: 302-314.
2. David Müzel S, Bonhin EP, Guimarães NM, Guidi ES. Application of the finite element method in the analysis of composite materials: A review. Polymers. 2020; 12: 818.
3. Reis PN, Ferreira JA, Antunes FV, Costa JD. Flexural behaviour of hybrid laminated composites. Compos Part A. 2007; 38: 1612-1620.
4. Archanowicz E, Kowaluk G, Niedziński W, Beer P. Properties of particleboards made of biocomponents from fibrous chips for FEM modeling. BioResources. 2013; 8: 6220-6230.
5. Soriano J, Fiorelli J, Junior WE, Barbirato GH, Deldotti LR. Numerical modeling for adjustment of the equivalent moduli of elasticity of OSB layers estimated from experimental flexural rigidity. J Mater Res Technol. 2021; 14: 1630-1643.
6. Mohanty AK, Wibowo A, Misra M, Drzal LT. Effect of process engineering on the performance

of natural fiber reinforced cellulose acetate biocomposites. Compos Part A. 2004; 3: 363-370.
7. Ochi S. Development of high strength biodegradable composites using Manila hemp fiber and starch-based biodegradable resin. Compos Part A. 2006; 37: 1879-1883.
8. Shahzad A. Hemp fiber and its composites - A review. J Compos Mater. 2012; 46: 973-986.
9. Hu R, Lim JK. Fabrication and mechanical properties of completely biodegradable hemp fiber reinforced polylactic acid composites. J Compos Mater. 2007; 41: 1655-1669.
10. Placet V, Day A, Beaugrand J. The influence of unintended field retting on the physicochemical and mechanical properties of industrial hemp bast fibres. J Mater Sci. 2017; 52: 5759-5777.
11. Musio S, Müssig J, Amaducci S. Optimizing hemp fiber production for high performance composite applications. Front Plant Sci. 2018; 9: 1702.
12. Mwaikambo LY, Tucker N, Clark AJ. Mechanical properties of hemp-fibre-reinforced euphorbia composites. Macromol Mater Eng. 2007; 292: 993-1000.
13. Placet V. Characterization of the thermo-mechanical behaviour of hemp fibres intended for the manufacturing of high performance composites. Compos Part A. 2009; 40: 1111-1118.
14. El Houjeyri I, Thi VD, Oudjene M, Ottenhaus LM, Khelifa M, Rogaume Y. Coupled nonlinear-damage finite element analysis and design of novel engineered wood products made of oak hardwood. Eur J Wood Wood Prod. 2021; 79: 29-47.
15. O'Loinsigh C, Oudjene M, Shotton E, Pizzi A, Fanning P. Mechanical behaviour and 3D stress analysis of multi-layered wooden beams made with welded-through wood dowels. Compos Struct. 2012; 94: 313-321.
16. Tran VD, Oudjene M, Méausoone PJ. Experimental and numerical analyses of the structural response of adhesively reconstituted beech timber beams. Compos Struct. 2015; 119: 206-217.
17. del Coz Díaz JJ, Nieto PG, Rabanal FA, Biempica CB. Finite element analysis of thin-walled composite two-span wood-based loadbearing stressed skin roof panels and experimental validation. Thin Walled Struct. 2008; 46: 276-289.
18. Suo S, Bowyer JL. Modeling of strength properties of structural particleboard. Wood Fiber Sci. 1995; 27: 84-94.
19. Chen Z, Yan N, Sam-Brew S, Smith G, Deng J. Investigation of mechanical properties of sandwich panels made of paper honeycomb core and wood composite skins by experimental testing and finite element (FE) modelling methods. Eur J Wood Wood Prod. 2014; 72: 311-319.
20. Warguła Ł, Wojtkowiak D, Kukla M, Talaśka K. Symmetric nature of stress distribution in the elastic-plastic range of Pinus L. pine wood samples determined experimentally and using the finite element method (FEM). Symmetry. 2021; 13: 1-30.
21. Dechaumphai P, Sucharitpwatskul S. Finite element analysis with ANSYS workbench. Oxford, U.K.: Alpha Science International Limited; 2018.
22. Bhavikatti SS. Finite element analysis.New Delhi, India: New Age International (P) Limited; 2005; ISBN (13): 978-81-224-2524-6.
23. Tankut N, Tankut AN, Zor M. Finite element analysis of wood materials. Drv Ind. 2014; 65: 159-171.
24. Kretschmann D. Mechanical properties of wood. US Department of Agriculture; Forest Service, Forest Products Laboratory; 2010.
25. Hunt JF. 3D engineered fiberboard: Finite element analysis of a new building product. 2004 International ANSYS Conference; 2004; Pittsburg, PA. Nation Forest Service Library.
26. Iraola B, Cabrero JM, Basterrechea-Arévalo M, Gracia J. A geometrically defined stiffness

contact for finite element models of wood joints. Eng Struct. 2021; 235: 112062.
27. Mackerle J. Finite element analyses in wood research: A bibliography. Wood Sci Technol. 2005; 39: 579-600.
28. Kaygin B, Yorur H, Uysal B. Simulating strength behaviors of corner joints of wood constructions by using finite element method. Wood Ind. 2016; 67: 133-140.
29. Malik MH, Arif AF. ANN prediction model for composite plates against low velocity impact loads using finite element analysis. Compos Struct. 2013; 101: 290-300.
30. Pousette A. Finite element analysis and test of joint at the center pole of a wooden spiral stair. For Prod J. 2007; 57: 25-29.
31. del Coz Díaz JJ, Nieto PG, Martínez-Luengas AL, Domínguez FS, Hernández JD. Non-linear numerical analysis of plywood board timber connections by DOE-FEM and full-scale experimental validation. Eng Struct. 2013; 49: 76-90.
32. Serrano E. A numerical study of the shear-strength-predicting capabilities of test specimens for wood–adhesive bonds. Int J Adhes Adhes. 2004; 24: 23-35.
33. Richard N, Yasumura M, Davenne L. Prediction of seismic behavior of wood-framed shear walls with openings by pseudodynamic test and FE model. J Wood Sci. 2003; 49: 145-151.
34. Pétrissans A, Hamada J, Chaouch M, Petrissans M, Gerardin P. Modeling and numerical simulation of wood torrefaction. Innov Woodwork Ind Eng Des., 2015; 5: 26-32.
35. Dahlblom O, Ormarsson S, Petersson H. Simulation of wood deformation processes in drying and other types of environmental loading. Ann For Sci. 1996; 53: 857-866.
36. Brooke AS, Langrish TA. The simulation of stresses and strains in the drying of Pinus radiata sapwood: The effects of board geometry. Comput Chem Eng. 1997; 21: 1271-1281.
37. Hansson L, Lundgren N, Antti AL, Hagman O. Finite element modeling (FEM) simulation of interactions between wood and microwaves. J Wood Sci. 2006; 52: 406-410.
38. Nicholls T, Crisan R. Study of the stress–strain state in corner joints and box-type furniture using Finite Element Analysis (FEA). Holz als Roh-und Werkst. 2002; 60: 66-71. DOI: 10.1007/S00107-001-0262-0.
39. Ilic S, Hackl K. Application of the multiscale FEM to the modeling of nonlinear multiphase materials. J Theor Appl Mech. 2009; 47: 537-551.
40. Jeong GY, Hindman DP. Modeling differently oriented loblolly pine strands incorporating variation of intraring properties using a stochastic finite element method. Wood Fiber Sci. 2010; 42: 51-61.
41. Kawecki B, Podgórski J. 3D ABAQUS simulation of bent softwood elements. Arch Civ Eng. 2020; 66: 323-337.
42. Fajdiga G, Rajh D, Nečemer B, Glodež S, Šraml M. Experimental and numerical determination of the mechanical properties of spruce wood. Forests. 2019; 10: 1140.
43. Dubois F, Chazal C, Petit C. Viscoelastic crack growth process in wood timbers: An approach by the finite element method for mode I fracture. Int J Fract. 2002; 113: 367-388.
44. Hu W, Wan H, Guan H. Size effect on the elastic mechanical properties of beech and its application in finite element analysis of wood structures. Forests. 2019; 10: 783.
45. Serrano E, Gustafsson J, Larsen HJ. Modeling of finger-joint failure in glued-laminated timber beams. J Struct Eng. 2001; 127: 914-921.
46. Tabiei A, Wu J. Three-dimensional nonlinear orthotropic finite element material model for wood. Compos Struct. 2000; 50: 143-149.

47. Clouston PL, Lam F. Computational modeling of strand-based wood composites. J Eng Mech. 2001; 127: 844-851.
48. Guan ZW, Zhu EC. Finite element modelling of anisotropic elasto-plastic timber composite beams with openings. Eng Struct. 2009; 31: 394-403.
49. Trivaudey F, Placet V, Guicheret-Retel V, Boubakar ML. Nonlinear tensile behaviour of elementary hemp fibres. Part II: Modelling using an anisotropic viscoelastic constitutive law in a material rotating frame. Compos Part A. 2015; 68: 346-355.
50. Oudjene M, Khelifa M. Finite element modelling of wooden structures at large deformations and brittle failure prediction. Mater Des. 2009; 30: 4081-4087.
51. Tran TT, Thi VD, Khelifa M, Oudjene M, Rogaume Y. A constitutive numerical modelling of hybrid-based timber beams with partial composite action. Constr Build Mater. 2018; 178: 462-472.
52. Mackenzie-Helnwein P, Eberhardsteiner J, Mang HA. A multi-surface plasticity model for clear wood and its application to the finite element analysis of structural details. Comput Mech. 2003; 31: 204-218.
53. Eslami H, Jayasinghe LB, Waldmann D. Nonlinear three-dimensional anisotropic material model for failure analysis of timber. Eng Fail Anal. 2021; 130: 105764.
54. Khorsandnia N, Valipour HR, Crews K. Nonlinear finite element analysis of timber beams and joints using the layered approach and hypoelastic constitutive law. Eng Struct. 2013; 46: 606-614.
55. Oudjene M, Khelifa M. Elasto-plastic constitutive law for wood behaviour under compressive loadings. Constr Build Mater. 2009; 23: 3359-3366.
56. Schmidt J, Kaliske M. Models for numerical failure analysis of wooden structures. Eng Struct. 2009; 31: 571-579.
57. Roszyk E, Moliński W, Fabisiak E. Radial variation of mechanical properties of pine wood (*Pinus sylvestris* L.) determined upon tensile stress. Wood Res. 2013; 58: 329-342.
58. Dahle AK, Sumitomo T, Instone S. Relationship between tensile and shear strengths of the mushy zone in solidifying aluminum alloys. Metall Mater Trans A. 2003; 34: 105-113.
59. Goulding B. Tensile strength, shear strength, and effective stress for unsaturated sand. Columbia: University of Missouri; 2006.
60. Nunziante L. Is there any relationship between shear strength and tensile strength of a metal? [Internet]. 2022. Available from: https://www.researchgate.net/post/Is-there-any-relationship-between-shear-strength-and-tensile-strength-of-a-metal/5e95868ee199e76db60dbf4f/citation/download.
61. Deutschman AD, Michels WJ, Wilson CE. Machine design; theory and practice. Prentice Hall; 1975.
62. Lam F, Lee G, Yan H, Gu J, Saravi AA. Structural performance of wood-based stair stringers. For Prod J. 2004; 54: 39-44.
63. Jauslin C, Pellicane PJ, Gutkowski RM. Finite-element analysis of wood joints. J Mater Civ Eng. 1995; 7: 50-58.
64. Xue J, Yuan Z, Ren G, Qi L, Zhang W, Wei J. Seismic performance of glued-laminated wood frame and frame brace structure: Experimental and finite element analysis. J Build Eng. 2022; 48: 103944.
65. Autengruber M, Lukacevic M, Wenighofer G, Mauritz R, Füssl J. Finite-element-based concept

to predict stiffness, strength, and failure of wood composite I-joist beams under various loads and climatic conditions. Eng Struct. 2021; 245: 112908.
66. Fu WL, Guan HY, Kei S. Effects of moisture content and grain direction on the elastic properties of beech wood based on experiment and finite element method. Forests. 2021; 12: 610.
67. Chui YH, Ni C, Jiang L. Finite-element model for nailed wood joints under reversed cyclic load. J Struct Eng. 1998; 124: 96-103.
68. Gilbert BP, Bailleres H, Zhang H, McGavin RL. Strength modelling of Laminated Veneer Lumber (LVL) beams. Constr Build Mater. 2017; 149: 763-777.
69. Santos P, Correia JR, Godinho L, Dias AM, Craveiro H. Experimental and numerical assessment of a cross-insulated timber panel solution. Eng Struct. 2021; 235: 112061.
70. Šmídová E, Kabele P, Šejnoha M. Finite element simulation of single edge notched timber arch. J Comput Appl Math. 2022; 400: 113676.
71. Wong ED, Yang P, Zhang M, Wang Q, Nakao T, Li KF, et al. Analysis of the effects of density profile on the bending properties of particleboard using finite element method (FEM). Eur J Wood Wood Prod. 2003; 61: 66-72.
72. Hao H, Chen W, Chen S, Meng Q. Finite element analysis of structural insulated panel with OSB skins against windborne debris impacts. Proceedings of 1st Pan-American congress on computational mechanics (PANACM); 2015; Buenos Aires, Argentina.
73. Labans E, Kaliniš K. Numerical versus experimental investigation of plywood sandwich panels with corrugated core. 3rd International Scientific Conference Civil Engineering ’11 Proceedings; 2011; Latvia University of Agriculture, Jelgava.
74. Mohammadabadi M, Jarvis J, Yadama V, Cofer W. Predictive models for elastic bending behavior of a wood composite sandwich panel. Forests. 2020; 11: 624.
75. Webo W, Masu LM, Nziu PK. Formulation of nanocellulosic fibres and particle fillers, and their mono and hybrid reinforced polymer composites. Mater Res Express. 2022; 9: 035404
76. Webo W, Masu LM, Nziu PK. Finite element analysis and experimental approaches of mono and hybrid nanocellulosic composites under tensile test. Mater Res Express. 2022; 9: 020001.
77. Gupta US, Dhamarikar M, Dharkar A, Tiwari S, Namdeo R. Study on the effects of fibre volume percentage on banana-reinforced epoxy composite by finite element method. Adv Compos Hybrid Mater. 2020; 3: 530-540.
78. Suryawanshi RT, Venkatachalam G, Vimalanand SV. Determination of stress intensity factor of banana fibre reinforced hybrid polymer matrix composite using Finite Element method. Period Polytech Mech Eng. 2016; 60: 180-184.
79. Silva LJ, Panzera TH, Christoforo AL, Durão LM, Lahr FA. Numerical and experimental analyses of biocomposites reinforced with natural fibres. Int J Mater Eng. 2012; 2: 43-49.
80. Shankar PS, Reddy KT, Sekhar VC, Sekhar VC. Mechanical performance and analysis of banana fiber reinforced epoxy composites. Int J Recent Trends Mech Eng. 2013; 1: 1-10.
81. Hariprasad T, Dharmalingam G, Raj PP. Study of mechanical properties of banana-coir hybrid composite using experimental and FEM techniques. J Mech Eng Sci. 2013; 4: 518-531.
82. Rajesh M, Srinag T, Prasanthi PP, Venkataraovenkatarao K. Finite element analysis of coir/banana fiber reinforced composite material. Int J Adv Res Mech Eng Technol. 2016; 2: 29-33.
83. Monzón MD, Paz R, Verdaguer M, Suárez L, Badalló P, Ortega Z, et al. Experimental analysis and simulation of novel technical textile reinforced composite of banana fibre. Materials. 2019; 12:

1134.

84. Ramesh M, Logesh R, Manikandan M, Kumar NS, Pratap DV. Mechanical and water intake properties of banana-carbon hybrid fiber reinforced polymer composites. Mater Res. 2017; 20: 365-376.
85. Alsoufi MS, Abdellah MY, Abdel-Jaber G, Fahmy HS, Hashem A. Finite element simulation of mechanical behaviour of sandwiched medium density fibre board. Am J Sci Technol. 2015; 2: 86-91.
86. Ganev S, Cloutier A, Gendron G, Beauregard R. Finite element modeling of the hygroscopic warping of medium density fiberboard. Wood Fiber Sci. 2005; 37: 337-354.